Inorganic Chemistry

including bioinorganic chemistry

February 3, 2014
Volume 53, Number 3
pubs.acs.org/IC

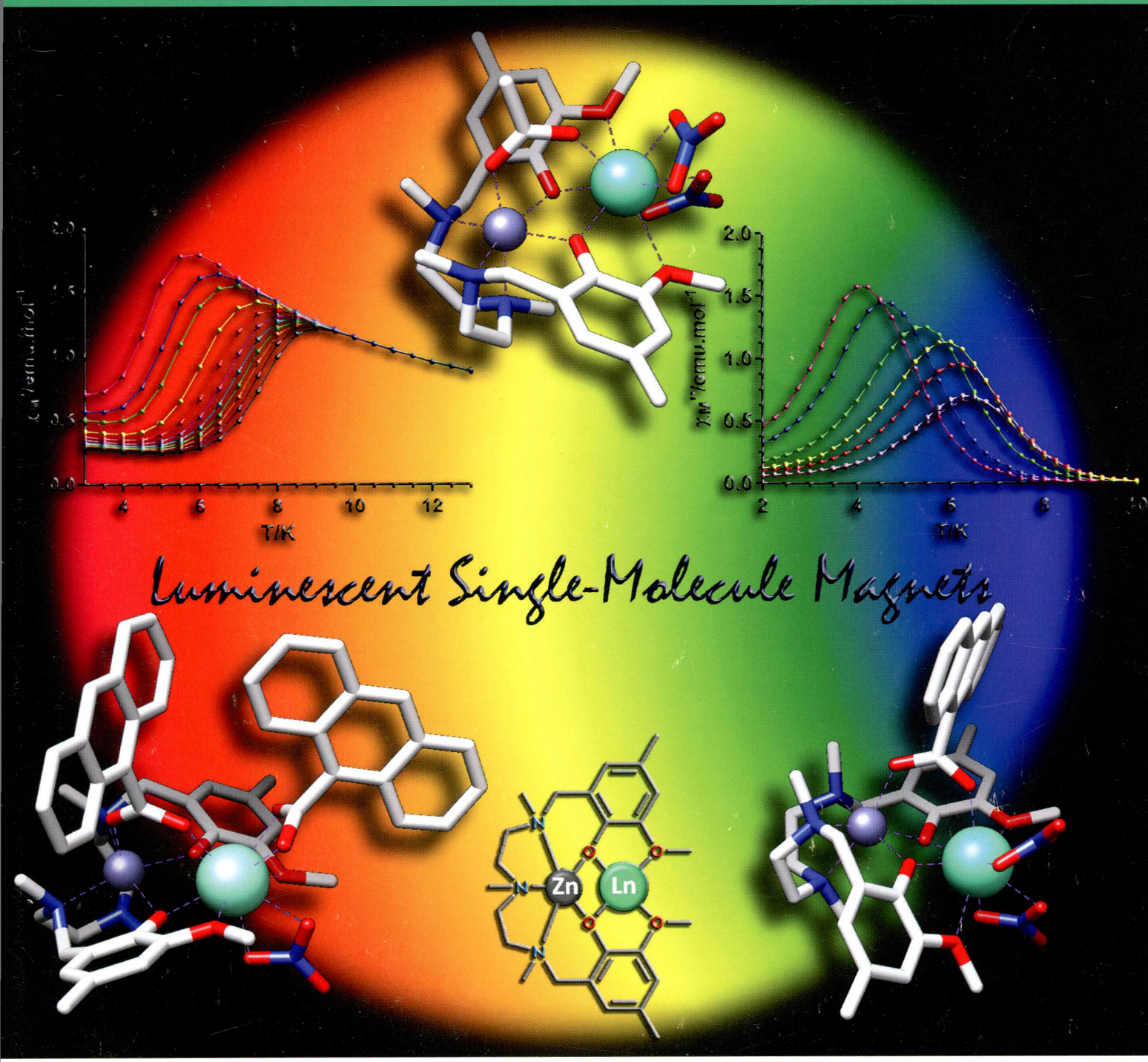

Inorganic Chemistry

FEBRUARY 3, 2014
VOLUME 53 ISSUE 3

INOCAJ 53(3) 1257–1790 (2014)
ISSN 0020-1669

ON THE COVER: An N_3O_4 nonadentate compartmental ligand allows the preparation of a family of luminescent $Zn^{II}Ln^{III}$ (Ln = Tb, Dy, Er, Nd, Yb) complexes. Among these, some Dy^{III} and Er^{III} complexes exhibit field-induced single-molecule-magnet behavior, thus behaving as dual magnetic–luminescent compounds. See M. A. Palacios, S. Titos-Padilla, J. Ruiz, J. M. Herrera, S. J. A. Pope, E. K. Brechin, and E. Colacio, p 1465. Dr. R. Cuesta, University of Jaén, Spain, is kindly acknowledged for his help in constructing the cover.

Communications

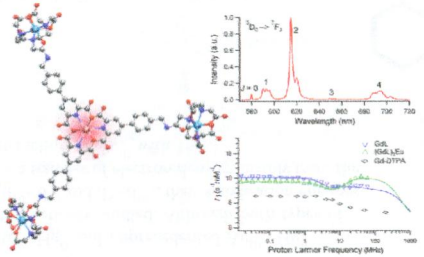

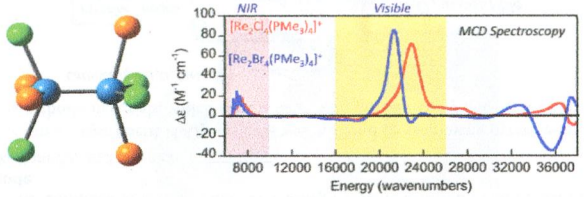

1263 S dx.doi.org/10.1021/ic402816a

Selective and Reusable Iron(II)-Based Molecular Sensor for the Vapor-Phase Detection of Alcohols

Anil D. Naik, Koen Robeyns, Christophe F. Meunier, Alexandre F. Léonard, Aurelian Rotaru, Bernard Tinant, Yaroslav Filinchuk, Bao Lian Su, and Yann Garcia*

An iron(II)-based molecular sensor capable of detecting methanol among an alcohol series is described. The sensing process is visually detectable, highly selective, fatigue-resistant, operable at room temperature, and reusable. Its crystal structure reveals the existence of channels that regulates host mobility and thus selectivity. Mössbauer spectroscopy relates the role of iron in this vapochromic spin-state change process. Real-time optical microscopic images further shed light on propagation of the methanol/spin state front.

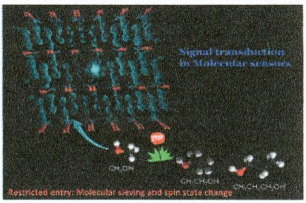

1266 S dx.doi.org/10.1021/ic4029113

$[ZnBi_4]^{3-}$ Pentagon in K_6ZnBi_5: Aromatic All-Metal Heterocycle

Qian Qin, Liujiang Zhou, Yi Wang, Ruili Sang, and Li Xu*

The first aromatic all-metal heterocycle $[ZnBi_4]^{3-}$ in the metallic salt K_6ZnBi_5 featuring an infinite sandwich structure has been established by the exactly planar $[ZnBi_4]^{3-}$ pentagon with six π electrons coupled with multiply bonded Zn–Bi and Bi–Bi bonds, multicentered π-conjugated bonding, and negative nucleus-independent chemical shift values. The metallic nature of K_6ZnBi_5 has been revealed by Pauli-type temperature-independent paramagnetism and theoretical analysis of the band structure and total/partial density of states.

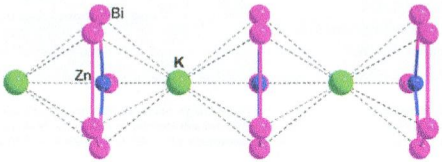

1269 S dx.doi.org/10.1021/ic402941z

Formation of Novel T-Shaped NNN Ligands via Rare-Earth Metal-Mediated Si–H Activation

Denis Bubrin and Mark Niemeyer*

Reactions of silylamides $[Ln\{N(SiHMe_2)_2\}_3(thf)_2]$ with sterically crowded aromatic amines $ArNH_2$ (Ar = Dmp, 2,6-$Mes_2C_6H_3$ with Mes = 2,4,6-$Me_3C_6H_2$; Ar* = 2,6-$Trip_2C_6H_3$ with Trip = 2,4,6-$i Pr_3C_6H_2$) afforded via a template reaction the formation of new tridentate ligand systems, and depending on the size of Ar, either derived complexes of composition $[LnN\{SiMe_2N(Dmp)\}_2]$ (Ln = Ce, Pr) or free protonated ligand $NH\{SiMe_2NH(Ar^*)\}_2$ were isolated.

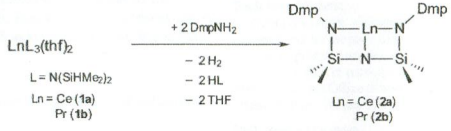

1272 dx.doi.org/10.1021/ic403008d

High Power Density of One-Compartment H_2O_2 Fuel Cells Using Pyrazine-Bridged $Fe[M^C(CN)_4]$ (M^C = Pt^{2+} and Pd^{2+}) Complexes as the Cathode

Yusuke Yamada,* Masaki Yoneda, and Shunichi Fukuzumi*

The high power density of one-compartment H_2O_2 fuel cells was achieved by employing pyrazine-bridged $Fe[M^C(CN)_4]$ (M^C = Pt or Pd) complexes as cathode materials, which have a large window size compared with cyanide-bridged complexes.

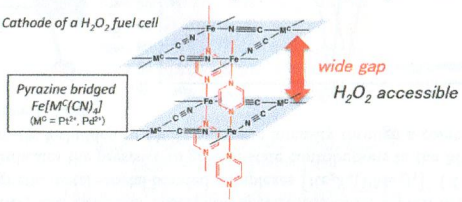

1275 dx.doi.org/10.1021/ic403036s

Experimental and Theoretical Comparison of the Metallophilicity between d^{10}–d^{10} Au^I–Hg^{II} and d^8–d^{10} Au^{III}–Hg^{II} Interactions

José M. López-de-Luzuriaga,* Miguel Monge, M. Elena Olmos, and David Pascual

Heteronuclear species displaying Au^I···Hg^{II} and unprecedented Au^{III}···Hg^{II} contacts have been prepared and theoretically studied. Although both types of interactions are formally different (d^{10}–d^{10} and d^8–d^{10}), their stabilization energies are quite similar as a consequence of a transfer of electron density, mainly from the phosphorus-donor ligand, upon interaction of Au^{III} with Hg^{II}.

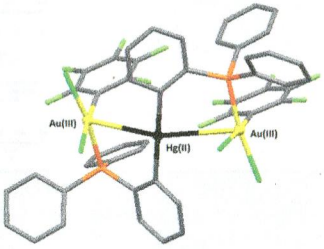

Articles

1278 dx.doi.org/10.1021/ic4009575

Formation Constants of Copper(II) Complexes with Tripeptides Containing Glu, Gly, and His: Potentiometric Measurements and Modeling by Generalized Multiplicative Analysis of Variance

Rima Raffoul Khoury, Gordon J. Sutton, Diako Ebrahimi, and D. Brynn Hibbert*

Each of the 27 combinations of the tripeptide formed from E, G, and H has been complexed with copper(II) and its formation constants of possible species measured by alkali titration. Generalized multiplicative analysis of variance (GEMANOVA) of logβ values shows interactions between residues can model the formation constants. Visible spectrometry confirmed the presence of dimers for HHE and HHG as well as bis compexes CuL_2 for complexes with (E/G)-H-(E/G) and $Cu(HL)_2$ with H-(E/G)-(E/G).

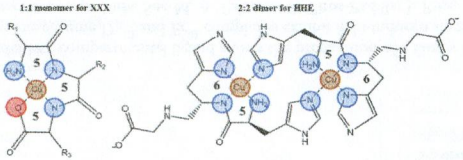

1288 dx.doi.org/10.1021/ic4012197

Synthesis and Properties of the Cyano Complex of Oxo-Centered Triruthenium Core $[Ru_3(\mu_3\text{-}O)(\mu\text{-}CH_3COO)_6(pyridine)_2(CN)]$

Hua-Xin Zhang,* Yoichi Sasaki,* Yi Zhang, Shen Ye, Masatoshi Osawa, Masaaki Abe, and Kohei Uosaki

A new oxo-centered triruthenium(III) complex with cyanide as the terminal ligand has been prepared and characterized. The redox potentials of two processes of the cyanide complex are even more negative than those of the pyridine-containing complex. Molecular orbital calculations revealed that the cyano-coordinated triruthenium unit has a delocalized electronic structure, while the corresponding CO-containing complex takes a localized structure due to the strong π-back donation to CO.

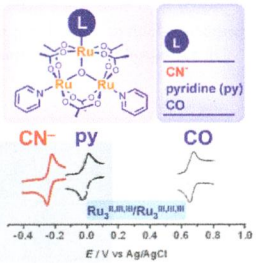

1295 dx.doi.org/10.1021/ic401484d

Tetranuclear Hetero-Metal $[Co^{II}_2Ln^{III}_2]$ (Ln = Gd, Tb, Dy, Ho, La) Complexes Involving Carboxylato Bridges in a Rare μ_4–η^2:η^2 Mode: Synthesis, Crystal Structures, and Magnetic Properties

Sk Md Towsif Abtab, Mithun Chandra Majee, Manoranjan Maity, Ján Titiš, Roman Boča,* and Muktimoy Chaudhury*

A series of 3d–4f heterometal complexes $[Co^{II}_2(L)_2(PhCOO)_2Ln^{III}_2(hfac)_4]$ (**1**–**5**) with $Co^{II}_2Ln^{III}_2$ (Ln = Gd, Tb, Dy, Ho, and La) cores and their $[Zn^{II}_2(L)_2(PhCOO)_2Dy^{III}_2(hfac)_4]$ analog (**6**) have been synthesized following a single-pot protocol. The metal centers in these isostructural compounds are connected by a pair of bridging carboxylato ligands in a rare μ_4–η^2:η^2 mode, providing antiferromagnetic couplings among the metal centers. Slow magnetic relaxation has been observed in the $[Co^{II}_2Dy^{III}_2]$ and $[Zn^{II}_2Dy^{III}_2]$ compounds showing a SMM behavior.

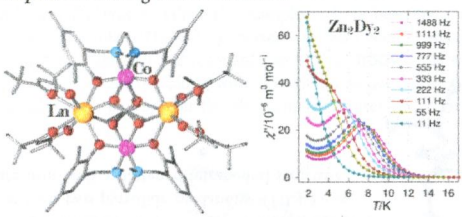

1307 dx.doi.org/10.1021/ic401701z

Water Oxidation Catalyzed by Mononuclear Ruthenium Complexes with a 2,2′-Bipyridine-6,6′-dicarboxylate (bda) Ligand: How Ligand Environment Influences the Catalytic Behavior

Robert Staehle, Lianpeng Tong, Lei Wang, Lele Duan, Andreas Fischer, Mårten S. G. Ahlquist,* Licheng Sun,* and Sven Rau*

A new water oxidation catalyst $[Ru^{III}(bda)(mmi)(OH_2)](CF_3SO_3)$ (**2**, H_2bda = 2,2′-bipyridine-6,6′-dicarboxylic acid; mmi = 1,3-dimethylimidazolium-2-ylidene) containing an axial N-heterocyclic carbene ligand and one aqua ligand was synthesized and fully characterized. While analogous Ru-bda water oxidation catalysts $[Ru(bda)L_2]$ (L = pyridyl ligands) are supposed to catalyze water oxidation through a bimolecular coupling pathway, our study points out that **2**, surprisingly, undergoes a single-site water nucleophilic attack (acid–base) pathway.

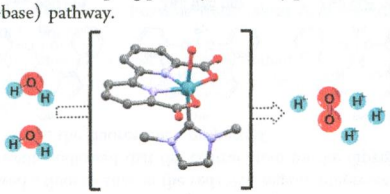

1320 dx.doi.org/10.1021/ic401928m

Formation of Coordination Polymers or Discrete Adducts via Reactions of Gadolinium(III)–Copper(II) 15-Metallacrown-5 Complexes with Polycarboxylates: Synthesis, Structures and Magnetic Properties

Anna V. Pavlishchuk, Sergey V. Kolotilov,* Matthias Zeller, Laurence K. Thompson, and Anthony W. Addison*

The X-ray structures of five complexes obtained from a hexanuclear Gd(III)–Cu(II) 15-metallacrown-5 and various polycarboxylates are reported. Two different models for simulating the magnetic properties of these 15-metallacrown-5 complexes are proposed and values for the exchange interactions are calculated for the first time.

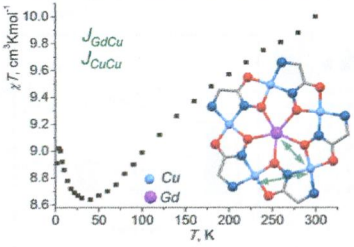

1331 dx.doi.org/10.1021/ic402015q

Functional Metal–Organic Frameworks via Ligand Doping: Influences of Ligand Charge and Steric Demand

Cheng Wang, Demin Liu, Zhigang Xie, and Wenbin Lin*

Three sterically demanding Ir/Ru phosphor-based dicarboxylate ligands of varying charges were systematically doped into the known IRMOF-9/-10 structures. The doped systems exhibit a strong tendency of adopting neutral framework structures, with the maximum ligand doping levels depending on the charge of the ligands. Our findings indicate important roles of steric demand and charge balance on ligand doping in metal–organic frameworks.

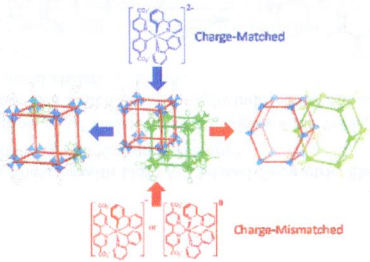

1339 dx.doi.org/10.1021/ic402082m

Intraligand Charge-Transfer Excited States in Re(I) Complexes with Donor-Substituted Dipyridophenazine Ligands

Christopher B. Larsen, Holly van der Salm, Charlotte A. Clark, Anastasia B. S. Elliott, Michael G. Fraser, Raphael Horvath, Nigel T. Lucas, Xue-Zhong Sun, Michael W. George,* and Keith C. Gordon*

Re(I) complexes with amine-appended dipyridophenazine donor–acceptor systems are reported. The optical and excited state properties are dominated by ILCT transitions. These systems are characterized by electrochemistry, electronic absorption spectroscopy, variable temperature and variable solvent emission spectroscopy, resonance Raman spectroscopy, resonance Raman excitation profiles, transient absorbance and emission spectroscopy, and time-resolved infrared spectroscopy.

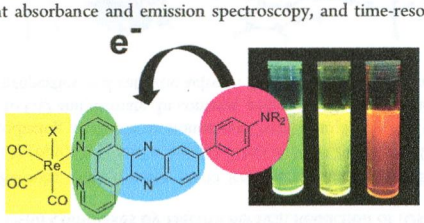

1355 S dx.doi.org/10.1021/ic402116j

Red/Near-Infrared Luminescence Tuning of Group-14 Element Complexes of Dipyrrins Based on a Central Atom

Masaki Yamamura, Marcel Albrecht, Markus Albrecht, Yoshinobu Nishimura, Tatsuo Arai, and Tatsuya Nabeshima*

We report the synthesis, structure, and photophysical properties of germanium and stannane complexes of the N2O2-type tetradentate dipyrrin, **L·Ge** and **L·Sn**, which are heavier analogues of the previously reported dipyrrin silicon complex, **L·Si**. All complexes **L·Si**, **L·Ge**, and **L·Sn** showed a fluorescence in the red/NIR region. Fluorescence quantum yields of **L·Ge** and **L·Sn** are higher than that of **L·Si**. These results indicated that the central atom on the dipyrrin complexes contributes not only to the geometry difference but also to tuning the fluorescence properties.

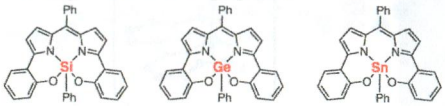

λ_{flu}: 650 nm, Φ : 2.8% | λ_{flu}: 675 nm, Φ : 12% | λ_{flu}: 664 nm, Φ : 22%

1361 S dx.doi.org/10.1021/ic402120r

Probing the Steric and Electronic Characteristics of a New Bis-Pyrrolide Pincer Ligand

Nobuyuki Komine, René W. Buell, Chun-Hsing Chen, Alice K. Hui, Maren Pink, and Kenneth G. Caulton*

A new diprotic and potentially redox active pincer ligand, H_2L, with pyrrrole rings attached to both ortho sites of a pyridine, forms LM(NCPh) for M = Pd, Pt. The molecule (HL)ZnEt binds *p*-dimethylaminopyridine (DMAP) to give four-coordinate LZn(DMAP). Electrochemistry shows three oxidation processes, which is interpreted to involve at least two pyrrolide oxidations. $(HL)_2Fe$ is shown to contain four-coordinate iron with a flattened-tetrahedral structure.

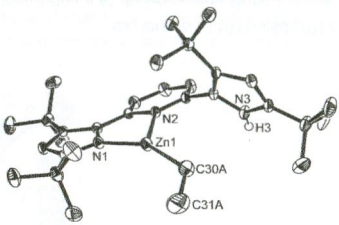

1370 S dx.doi.org/10.1021/ic402150k

Novel Trisphosphine Ligand Containing 1,3,5-Triazine Core, [2,4,6-$C_3N_3\{C_6H_4PPh_2$-*p*$\}_3$]: Synthesis and Transition Metal Chemistry

Susmita Naik, Maruthai Kumaravel, Joel T. Mague, and Maravanji S. Balakrishna*

This paper describes the synthesis and transition metal chemistry of a new trisphosphine with 1,3,5-triazine core, [2,4,6-$C_3N_3\{C_6H_4PPh_2$-*p*$\}_3$].

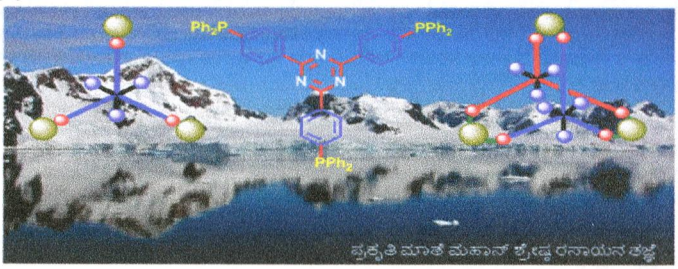

1382 S dx.doi.org/10.1021/ic402146t

Solvent-Dependent Formation of Os(0) Complexes by Electrochemical Reduction of [Os(CO)(2,2′-bipyridine)(L)Cl_2]; L = Cl^-, PrCN

Joanne Tory, Lisa King, Antonios Maroulis, Matti Haukka, Maria José Calhorda, and František Hartl*

The Os(II) complexes *mer*-[Os(CO) (bpy)Cl_3]$^-$ and *trans*(Cl)-[Os(CO)(PrCN) (bpy)Cl_2] (PrCN = butyronitrile) undergo irreversible reduction in PrCN, producing a soluble mononuclear Os(0) complex [Os(CO) (PrCN)(bpy)]^n (n = 0, −1) capable of catalytic CO_2 reduction to CO and formate. In contrast, polymeric Os(0) products are obtained in THF and also in MeCN, exhibiting different redox properties and catalytic activity. A comparison with related Ru and Os literature species is presented.

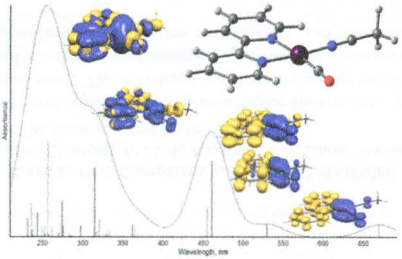

1397 S dx.doi.org/10.1021/ic402221x

Characterization of a Photoswitching Chelator with Light-Modulated Geometric, Electronic, and Metal-Binding Properties

Andrew T. Franks, Degao Peng, Weitao Yang, and Katherine J. Franz*

HAPI is a hydrazone-containing transition metal chelator that undergoes a reversible, photoinduced *E*-to-*Z* configurational switch about the hydrazone double bond. This switch allows for light-induced modification and restoration of molecular shape, electronic conjugation, and transition metal chelation efficacy.

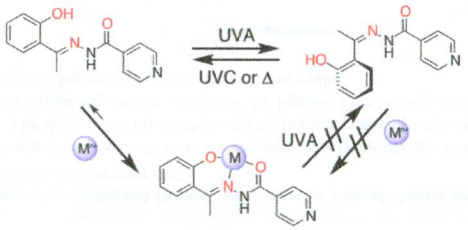

1406 dx.doi.org/10.1021/ic402119s

Structural, Spectral, and Electrochemical Properties of Nickel(II), Copper(II), and Zinc(II) Complexes Containing 12-Membered Pyridine- and Pyridol-Based Tetra-aza Macrocycles

Kimberly M. Lincoln, Michael E. Offutt, Travis D. Hayden, Ryker E. Saunders, and Kayla N. Green*

A series of Ni(II), Cu(II), and Zn(II) complexes have been produced and characterized from pyridine- or pyridol-containing N-heterocyclic amine ligands. The characterization provided insight into the Lewis acidity imparted by the ligand set in relation to the presence and position of the -OH group on the aromatic ring.

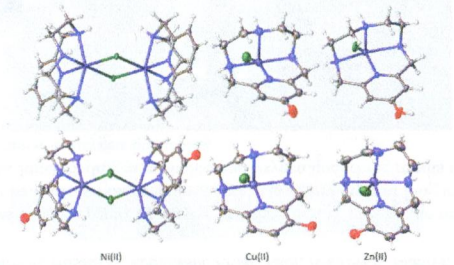

1417 dx.doi.org/10.1021/ic402304e

Synthesis, Spectral Characterization, Structures, and Oxidation State Distributions in [(corrolato)Fe^{III}(NO)]^n (n = 0, +1, −1) Complexes

Woormileela Sinha, Naina Deibel, Hemlata Agarwala, Antara Garai, David Schweinfurth, Chandra Shekhar Purohit, Goutam Kumar Lahiri,* Biprajit Sarkar,* and Sanjib Kar*

Two novel *trans*-A_2B-corroles and three [(corrolato){FeNO}^{6}] complexes have been prepared and characterized by various spectroscopic techniques. Two of the [(corrolato){FeNO}^{6}] species have also been characterized by single crystal X-ray crystallography. UV−vis, IR, and electron paramagnetic resonance spectroelectrochemical studies of all the three nitrosyl derivatives were carried out. Spectroelectrochemistry along with density functional theory (DFT) and time-dependent-DFT calculations have been cused in combination to decipher the electronic structures of the one-electron oxidized and reduced forms.

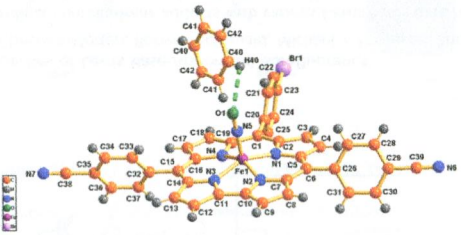

1430 dx.doi.org/10.1021/ic402358s

Photoreduction of Pt(IV) Halo-Hydroxo Complexes: Possible Hypohalous Acid Elimination

Lasantha A. Wickramasinghe and Paul R. Sharp*

Photolysis of Pt(IV) halo-hydroxo complexes causes net *cis*-photoelimination of HOX and solvent or alkene oxidation probably initiated by hydroxo radical formation from the lowest-energy triplet.

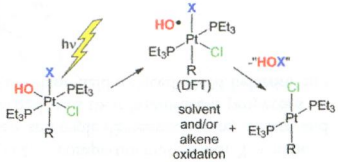

1443 (S) dx.doi.org/10.1021/ic402363s

Synthesis, Crystal and Electronic Structure of the Quaternary Magnetic $EuTAl_4Si_2$ (T = Rh and Ir) Compounds

Arvind Maurya, Arumugam Thamizhavel, Alessia Provino, Marcella Pani, Pietro Manfrinetti, Durga Paudyal, and Sudesh Kumar Dhar*

Two new ordered truly quaternary compounds $EuRhAl_4Si_2$ and $EuIrAl_4Si_2$ has been found to be stabilized in Al–Si eutectic flux, further establishing the power of crystal growth by solvent technique to discover new materials. These compounds crystallize in the ordered variant of KCu_4S_3 structure type as confirmed by single crystal XRD. A DFT calculation supports the stability of the ordered phase for these compounds.

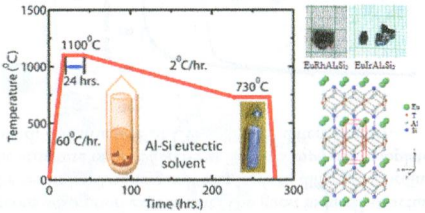

1449 (S) dx.doi.org/10.1021/ic402366x

Interaction of Antidiabetic Vanadium Compounds with Hemoglobin and Red Blood Cells and Their Distribution between Plasma and Erythrocytes

Daniele Sanna, Maria Serra, Giovanni Micera, and Eugenio Garribba*

Antidiabetic $V^{IV}O$ drugs with VOL_2 composition penetrate the erythrocyte membrane through passive diffusion. In the red blood cells, these compounds interact with hemoglobin (Hb) and undergo biotransformation to give binary species $V^{IV}O$–Hb and ternary complexes *cis*-VOL_2(Hb) with the equatorial coordination of a His–N of Hb polypeptide chain. These processes can significantly influence the mechanism of transport and effectiveness of V drugs.

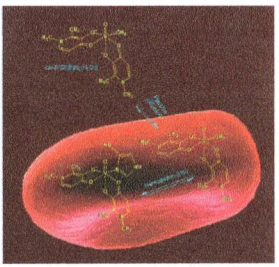

1465 S dx.doi.org/10.1021/ic402597s

Bifunctional $Zn^{II}Ln^{III}$ Dinuclear Complexes Combining Field Induced SMM Behavior and Luminescence: Enhanced NIR Lanthanide Emission by 9-Anthracene Carboxylate Bridging Ligands

María A. Palacios, Silvia Titos-Padilla, José Ruiz, Juan Manuel Herrera,* Simon J. A. Pope, Euan K. Brechin, and Enrique Colacio*

A series of $Zn^{II}Ln^{III}$ dinuclear complexes of formula $[Zn(\mu\text{-}L)(\mu\text{-}X)Ln(NO_3)_2]$ (H_2L = compartmental ligand; X = none, NO_3^-, OAc^-, and 9-An; Ln^{III} = Dy, Tb, Er, Nd, Yb) having double diphenoxo bridges and triple diphenoxonitrate, acetate, and 9-anthracene carboxylate bridges have been structurally and magnetically characterized, and their luminescent properties studied in the vis and NIR regions. Two Dy^{III} complexes and two Er^{III} complexes combine field-induced SMM behavior and luminescent properties.

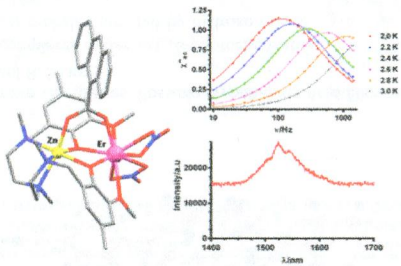

1475 S dx.doi.org/10.1021/ic402408t

Synthesis and Luminescent Properties of Lewis Base-Appended Borafluorenes

Christopher J. Berger, Gang He, Christian Merten, Robert McDonald, Michael J. Ferguson, and Eric Rivard*

A new class of luminescent 4-coordinate borafluorene adducts with various Lewis bases have been prepared and characterized, using a combination of experimental and computational methods.

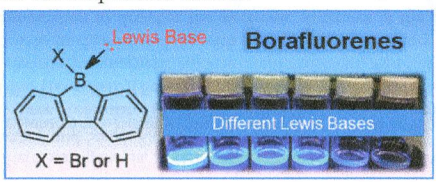

1487 S dx.doi.org/10.1021/ic402411g

$[Ir(N^N^N)(C^N)L]^+$: A New Family of Luminophores Combining Tunability and Enhanced Photostability

Danielle N. Chirdon, Wesley J. Transue, Husain N. Kagalwala, Aman Kaur, Andrew B. Maurer, Tomislav Pintauer, and Stefan Bernhard*

A family of iridium complexes has been prepared by varying the three ligand sites in the relatively unexplored structure $[Ir(N^N^N)(C^N)L]^+$. The new complexes exhibit interesting electrochemistry and long-lived phosphorescence which are readily tuned via ligand alterations. Initial hydrogen evolution and oxygen quenching results reveal highly desirable properties including photostability and resistance to oxygen quenching.

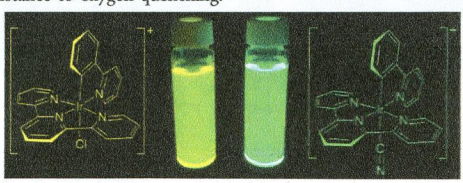

1500 dx.doi.org/10.1021/ic402467g

Structural Diversity and Photoluminescent Properties of Zinc Benzotriazole-5-carboxylate Coordination Polymers

Juan Liu, Hua-Bin Zhang, Yan-Xi Tan, Fei Wang, Yao Kang, and Jian Zhang*

Four-coordinate polymers were synthesized in elaborately designed experiments under solvothermal conditions. One of them is a chiral framework constructed with only a rigid ligand. The results demonstrate that the structural diversity of these four complexes with similar structures can be controlled by reasonable selection of auxiliary ligands.

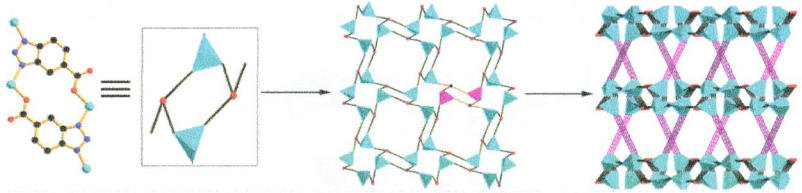

1507 dx.doi.org/10.1021/ic402476b

Selective DNA Purine Base Photooxidation by Bis-terdentate Iridium(III) Polypyridyl and Cyclometalated Complexes

Alexandre Jacques, Andrée Kirsch-De Mesmaeker, and Benjamin Elias*

Two luminescent bis-terdentate iridium(III) complexes with polypyridyl and cyclometalated ligands have been prepared and their spectroscopic and electrochemical properties studied. In the presence of mono- or polynucleotides, a photoinduced electron-transfer process from a DNA purine base (i.e. guanine or adenine) to the excited complex is shown through luminescence quenching experiments.

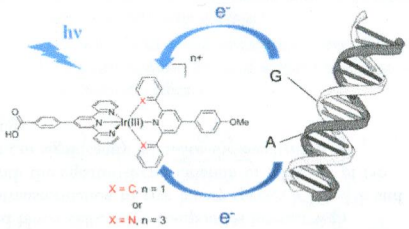

1513 dx.doi.org/10.1021/ic4024844

In Situ Observation of Gating Phenomena in the Flexible Porous Coordination Polymer $Zn_2(BPnDC)_2(bpy)$ (SNU-9) in a Combined Diffraction and Gas Adsorption Experiment

Volodymyr Bon, Irena Senkovska, Dirk Wallacher, Daniel M. Többens, Ivo Zizak, Ralf Feyerherm, Uwe Mueller, and Stefan Kaskel*

The intrinsic structural dynamic during adsorption/desorption of CO_2 at 195 K and N_2 at 77 K on SNU-9 was investigated by powder X-ray analysis and simultaneous adsorption experiment. The guest induced structural transformation is caused mainly by Zn−O bond rearrangement in the secondary building unit that leads to different coordination geometries of Zn atoms in as made and activated compounds. The structure of N_2@SNU-9 at 77 K (compound completely filled with nitrogen) is identical to the structure of as made compound; the structure of CO_2@SNU-9 differs slightly.

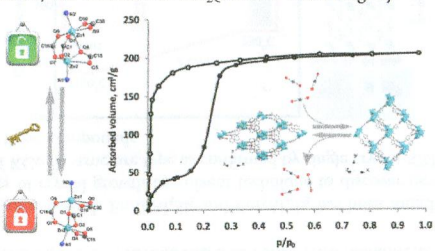

1521 dx.doi.org/10.1021/ic402494m

Nanocage Structure Derived from Sulfonated β-Cyclodextrin Intercalated Layered Double Hydroxides and Selective Adsorption for Phenol Compounds

Xiangyu Xue, Qingyang Gu, Guohua Pan, Jie Liang, Gailing Huang, Genban Sun, Shulan Ma,* and Xiaojing Yang

The intercalation of sulfonated β-cyclodextrin into LDHs produced nanocage structure, which revealed selective adsorption property for phenol compounds.

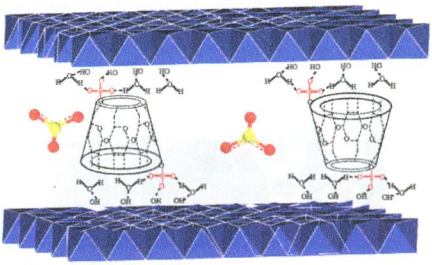

1530 dx.doi.org/10.1021/ic402524z

Extension of Novel Lanthanide Luminescent Mesoporous Nanostructures to Detect Fluoride

Zhan Zhou, Yuhui Zheng, and Qianming Wang*

A novel polydentate type ligand derived from N^2,N^6-bis(4,4-diethoxy-9-oxo-3-oxa-8,10-diaza-4-siladodecan-12-yl)pyridine-2,6-dicarboxamide (**L**) has been designed, and it played essential roles in the assembly of new organic−inorganic functional materials.

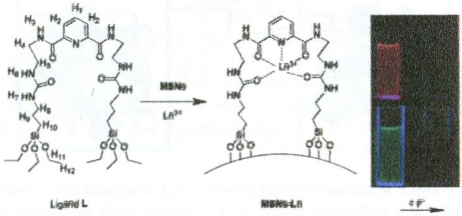

1537 dx.doi.org/10.1021/ic402530w

Reversible Switching of Coordination Mode of ansa bis(Amidinate) Ligand in Ytterbium Complexes Driven by Oxidation State of the Metal Atom

Aleksei O. Tolpygin, Anton V. Cherkasov, Georgii K. Fukin, and Alexander A. Trifonov*

Ansa bis(amidinate) ligand $[C_6H_4\text{-}1,2\text{-}\{NC(t\text{-}Bu)N(2,6\text{-}Me_2C_6H_3)\}_2]^{2-}$ coordinates to Yb(II) in κ^1amide, η^6-arene mode, resulting in a bent bis(arene) structure, while the Yb(III) derivatives feature "classic" κ^2N,N′ mode. The redox reactions Yb(II)Yb(III) are reversibly accompanied by a change of coordination mode.

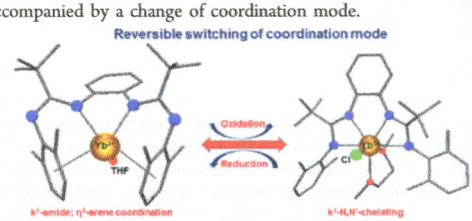

1544 Ⓢ dx.doi.org/10.1021/ic402538e

A Combined Computational and Spectroelectrochemical Study of Platinum-Bridged Bis-Triarylamine Systems

Matthias Parthey, Kevin B. Vincent, Manuel Renz, Phil A. Schauer, Dmitry S. Yufit, Judith A. K. Howard, Martin Kaupp,* and Paul J. Low*

The character of the electronic transitions in "inverted" mixed-valence complexes (organic electrophores, metal-based bridge) have been determined from a combination of spectroscopic measurement and BLYP35-COSMO-based density functional theory (DFT) calculations. The successful modeling of the charge distribution within the system demonstrates the utility of the BLYP35-COSMO protocol as a tool for use in the study of intramolecular charge transfer properties in mixed-valence complexes.

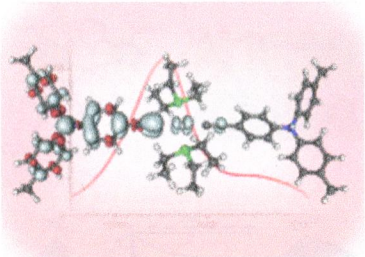

1555 Ⓢ dx.doi.org/10.1021/ic4025519

Redox Reactions of [FeFe]-Hydrogenase Models Containing an Internal Amine and a Pendant Phosphine

Dehua Zheng, Mei Wang,* Lin Chen, Ning Wang, and Licheng Sun*

Redox reactions of diiron dithiolate complexes with a pendant phosphine and an internal amine were studied, giving a series of new $Fe^{II}Fe^{I}$, $Fe^{II}Fe^{II}$, and $Fe^{I}Fe^{I}$ complexes relavant to H_{ox}, H_{ox}^{CO}, and H_{red} states of the [FeFe]-hydrogenase active site.

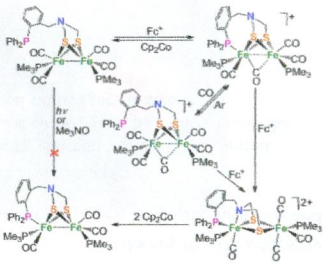

1562 Ⓢ dx.doi.org/10.1021/ic402570b

Raman Spectroscopic and ESI-MS Characterization of Uranyl Peroxide Cage Clusters

Brendan T. McGrail, Ginger E. Sigmon, Laurent J. Jouffret, Christopher R. Andrews, and Peter C. Burns*

Uranyl–peroxo–uranyl dihedral bond angles in cage clusters and the position of the Raman band of the symmetric stretching mode of the peroxo ligand are correlated. Electrospray ionization mass spectra of uranyl peroxide cage clusters permit detection and extraction of information about their bonding and composition without crystallization.

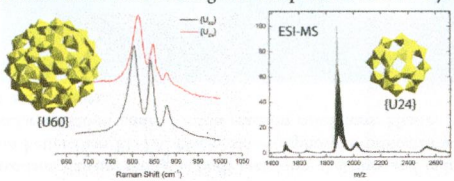

1570 S dx.doi.org/10.1021/ic402613z

Kinetic and Mechanistic Studies on the Reaction of the Vitamin B_{12} Complex Aquacobalamin with the HNO Donor Angeli's Salt: Angeli's Salt and HNO React with Aquacobalamin

Harishchandra Subedi, Hanaa A. Hassanin, and Nicola E. Brasch*

Kinetic and mechanistic studies on the reaction between the vitamin B_{12} derivative aquacobalamin (H_2OCbl^+/HOCbl) and the HNO donor Angeli's salt show that aquacobalamin reacts directly with Angeli's salt, $HN_2O_3^-$, to form nitroxylcobalamin and nitrite at pH <9.90. At pH >10.80 the reaction instead switches predominantly to a mechanism in which spontaneous decomposition of Angeli's salt to give HNO and nitrite becomes the rate-determining step, followed by the rapid reaction between aquacobalamin and HNO/NO^- to again give NOCbl.

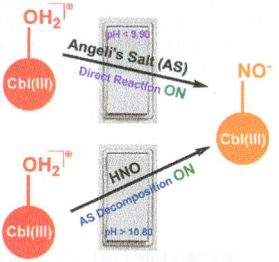

1578 dx.doi.org/10.1021/ic402616r

Control of L-type Ferrimagnetism by the Ce/Vacancy Ordering in the *A*-Site-Ordered Perovskite $Ce_{1/2}Cu_3Ti_4O_{12}$

Takashi Saito,* Ryuta Yamada, Clemens Ritter, Mark S. Senn, J. Paul Attfield, and Yuichi Shimakawa

A-site-ordered perovskite $Ce_{1/2}Cu_3Ti_4O_{12}$ crystallizes in two different forms, one with random and the other with ordered Ce/vacancy distribution at the *A* site of the prototype $AA'_3B_4O_{12}$ structure. Both phases form a G-type spin structure of Cu^{2+} spins below 24 K, although their magnetisms are quite different. The former undergoes a typical antiferromagnetic transition, whereas the latter shows an L-type ferrimagnetism. The unusual ferrimagnetism is a direct consequence of the Ce/vacancy ordering.

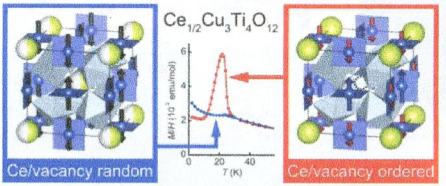

1585 S dx.doi.org/10.1021/ic402664n

Uranium(VI) Chemistry in Strong Alkaline Solution: Speciation and Oxygen Exchange Mechanism

Henry Moll, André Rossberg, Robin Steudtner, Björn Drobot, Katharina Müller, and Satoru Tsushima*

The combination of quantum-chemical calculations and X-ray absorption spectroscopy suggests the presence of the species $UO_3(OH)_3^{3-}$, which stimulates the "yl"–oxygen exchange.

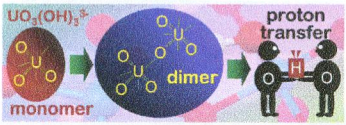

1594 dx.doi.org/10.1021/ic402671q

Nucleoside—2′,3′/3′,5′-Bis(thio)phosphate Analogues Are Promising Antioxidants Acting Mainly via Cu^{+}/Fe^{2+} Ion Chelation

Bosmat Levi Hevroni, Alon Haim Sayer, Eliav Blum, and Bilha Fischer*

A series of adenine/guanine 2′,3′- or 3′,5′-bisphosphate (A/G−BP) inhibited OH. production in a Fe^{2+}-H_2O_2 system, 2- and 5-fold more effectively than EDTA and ADP, respectively. Adenine/guanine 2′,3′- or 3′,5′-bisphosphorothioates (A/G−BP−S) exhibited a dual antioxidant activity, acting as both metal-ion chelators and radical scavengers. A−P−S inhibited Cu^{+}-induced H_2O_2 decomposition better than EDTA. Nucleoside−bisphosphorothioates were weaker inhibitors than bisphosphates, due to intramolecular oxidation under Fenton reaction conditions. Hence, A/G−BP are potentially useful as biocompatible and water-soluble antioxidants.

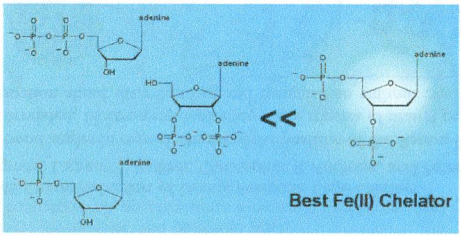

1606 dx.doi.org/10.1021/ic402673v

High Nuclearity (Octa-, Dodeca-, and Pentadecanuclear) Metal (M = Co^{II}, Ni^{II}) Phosphonate Cages: Synthesis, Structure, and Magnetic Behavior

Javeed Ahmad Sheikh, Amit Adhikary, Himanshu Sekhar Jena, Soumava Biswas, and Sanjit Konar*

The synthesis and the structural and magnetic characterizations of five high-nuclearity phosphonate cages is reported. Structural investigation reveals some interesting geometrical features in the molecular cores. Magnetic studies reveal the presence of both antiferromagnetic and ferromagnetic interactions between the metal centers for all cages.

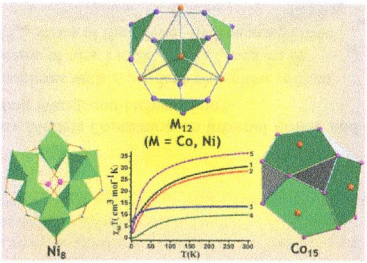

1614 Ⓢ dx.doi.org/10.1021/ic402675w

Trialkylphosphine-Stabilized Copper(I) Dialkylaluminum(III) Ethanedithiolate Complexes: Single-Source Precursors and a Novel Modification of Copper Aluminum Disulfide

Marcus Kischel, Gregor Dornberg, and Harald Krautscheid*

New organometallic copper(I) aluminum(III) complexes of the general formulas $[^{i}Pr_3PCuSC_2H_4SAlR_2]_2$ and $[(Me_3P)_4Cu][SC_2H_4SAlR_2]$ (R = Me, Et, ^{i}Pr, ^{t}Bu, vinyl) have been prepared and structurally characterized by X-ray diffraction. In thermolysis experiments, these complexes have been converted into the ternary semiconductor $CuAlS_2$. A yet-unknown hexagonal modification of $CuAlS_2$ has been identified in some thermolysis residues.

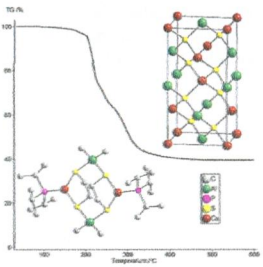

1624 dx.doi.org/10.1021/ic4026766

Superheavy Element Flerovium (Element 114) Is a Volatile Metal

Alexander Yakushev, Jacklyn M. Gates, Andreas Türler, Matthias Schädel, Christoph E. Düllmann,* Dieter Ackermann, Lise-Lotte Andersson, Michael Block, Willy Brüchle, Jan Dvorak, Klaus Eberhardt, Hans G. Essel, Julia Even, Ulrika Forsberg, Alexander Gorshkov, Reimar Graeger, Kenneth E. Gregorich, Willi Hartmann, Rolf-Dietmar Herzberg, Fritz P. Heßberger, Daniel Hild, Annett Hübner, Egon Jäger, Jadambaa Khuyagbaatar, Birgit Kindler, Jens V. Kratz, Jörg Krier, Nikolaus Kurz, Bettina Lommel, Lorenz J. Niewisch, Heino Nitsche, Jon Petter Omtvedt, Edward Parr, Zhi Qin, Dirk Rudolph, Jörg Runke, Brigitta Schausten, Erwin Schimpf, Andrey Semchenkov, Jutta Steiner, Petra Thörle-Pospiech, Juha Uusitalo, Maciej Wegrzecki, and Norbert Wiehl

The electronic structure of superheavy elements ($Z \geq 104$) and their chemical properties are dominated by relativistic effects. Recently two superheavy elements were recognized by the IUPAC and named *flerovium* (Fl, $Z = 114$) and *livermorium* (Lv, $Z = 116$). Fl is the heaviest element with which chemical experiments were performed. Here, we report on experiments that help answering the long-standing question whether Fl behaves rather like a noble gas or like a metal.

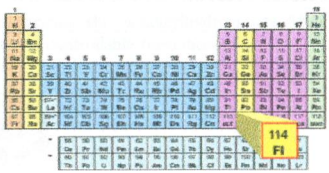

1630 Ⓢ dx.doi.org/10.1021/ic402987n

Transformation of Barium–Titanium Chloro–Alkoxide Compound to $BaTiO_3$ Nanoparticles by $BaCl_2$ Elimination

Magdalena Kosińska-Klähn, Łukasz John, Anna Drąg-Jarząbek, Józef Utko, Rafał Petrus, Lucjan B. Jerzykiewicz, and Piotr Sobota*

In this Article, we present how the molecular precursor of binary oxide material having an excess of alkali earth metal can be transformed to the highly phase pure $BaTiO_3$ perovskite. The advantage of this approach is that when barium-to-titanium stoichiometry forces spinel composition on the molecular level, it is possible to easily remove an excess of barium atoms through the substitution of triphenylacetate ligands in carboxy–alkoxide complex by chlorides and then simple $BaCl_2$ elimination after thermolysis.

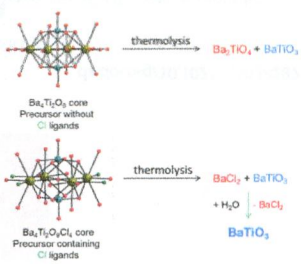

1637 Ⓢ dx.doi.org/10.1021/ic402701v

A Heteroleptic Bis(tridentate) Ruthenium(II) Platform Featuring an Anionic 1,2,3-Triazolate-Based Ligand for Application in the Dye-Sensitized Solar Cell

Stephan Sinn, Benjamin Schulze, Christian Friebe, Douglas G. Brown, Michael Jäger, Joachim Kübel, Benjamin Dietzek,* Curtis P. Berlinguette,* and Ulrich S. Schubert*

A new ruthenium(II) sensitizer platform featuring a readily prepared 1,2,3-triazolate-based tridentate ligand is reported. On account of the anionic 1,2,3-triazolates, the new sensitizer features a broad absorption of visible light, metal-to-ligand charge transfer transitions directed toward the anchoring ligand, relatively long excited-state lifetime, and redox potentials suitable for applications in the dye-sensitized solar cell. Accordingly, the new thiocyanate-free sensitizer achieves power-conversion efficiencies that approach the ones of a thiocyanate-containing benchmark sensitizer.

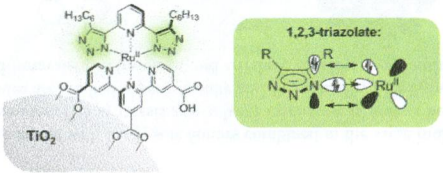

1646 Ⓢ dx.doi.org/10.1021/ic402767j

Boron-Dipyrromethene Based Reversible and Reusable Selective Chemosensor for Fluoride Detection

Sheri Madhu and Mangalampalli Ravikanth*

We have developed a benzimidazole substituted boron-dipyrromethene (BODIPY) based reversible and reusable fluorescent sensor, which showed remarkable selectively and specificity toward F^- ion.

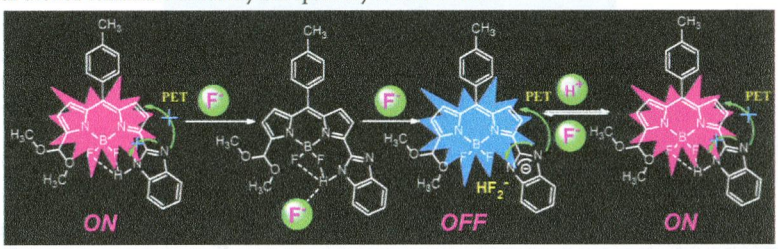

1654 Ⓢ dx.doi.org/10.1021/ic4027859

Divalent Heteroleptic Ytterbium Complexes – Effective Catalysts for Intermolecular Styrene Hydrophosphination and Hydroamination

Ivan V. Basalov, Sorin Claudiu Roşca, Dmitry M. Lyubov, Alexander N. Selikhov, Georgy K. Fukin, Yann Sarazin, Jean-François Carpentier,* and Alexander A. Trifonov*

New heteroleptic Yb(II)–amide species proved to be efficient precatalysts for the intermolecular hydrophosphination and hydroamination of styrene with diphenylphosphine, phenylphosphine, and pyrrolidine to give exclusively the anti-Markovnikov monoaddition product.

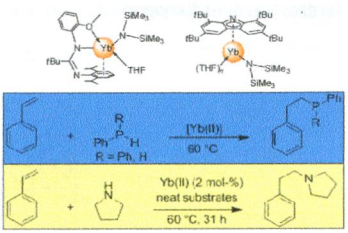

1662 S dx.doi.org/10.1021/ic402796k

DNA Condensing Effects and Sequence Selectivity of DNA Binding of Antitumor Noncovalent Polynuclear Platinum Complexes

Jaroslav Malina, Nicholas P. Farrell, and Viktor Brabec*

The noncovalent analogues of antitumor polynuclear platinum complexes are capable of inducing DNA condensation at more than 1 order of magnitude lower concentrations than conventional DNA condensing agents. This unique ability of the noncovalent polynuclear platinum complexes to condense DNA along with their sequence-specific DNA binding is proposed to contribute to mechanisms underlying their antitumor and cytotoxic activities.

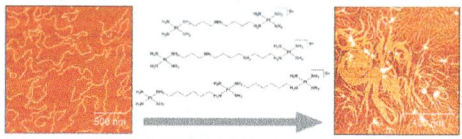

1672 S dx.doi.org/10.1021/ic4028282

Inhibitory Effect of Selenoprotein P on Cu^{+}/Cu^{2+}-Induced $A\beta_{42}$ Aggregation and Toxicity

Xiubo Du, Zhi Wang, Youbiao Zheng, Haiping Li, Jiazuan Ni, and Qiong Liu*

Copper in both oxidation states of Cu^{+} and Cu^{2+} promoted the aggregation and neurotoxicity of $A\beta_{42}$, which could be significantly restored by selenoprotein P.

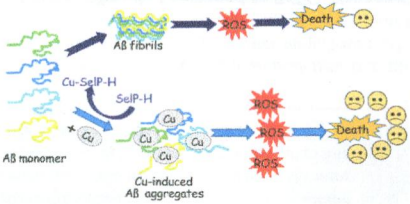

1679 S dx.doi.org/10.1021/ic4028332

Red-Emitting $[Ru(bpy)_2(N\text{-}N)]^{2+}$ Photosensitizers: Emission from a Ruthenium(II) to 2,2′-Bipyridine ^{3}MLCT State in the Presence of Neutral Ancillary "Super Donor" Ligands

Amlan K. Pal, Samik Nag, Janaina G. Ferreira, Victor Brochery, Giuseppina La Ganga, Antonio Santoro, Scolastica Serroni, Sebastiano Campagna,* and Garry S. Hanan*

A series of complexes containing bis(2,2′-bipyridine)ruthenium(II) and neutral ancilliary "super donor" ligands were synthesized and characterized. Their structural, electrochemical, and photophysical properties were studied and compared to those of tris(2,2′-bipyridine)ruthenium(II) and some reference compounds. Their properties were also modeled by density functional theory calculations, and trends were found vs the nature of the basicity of the heterocycle attached to the saturated aliphatic guanidium moiety.

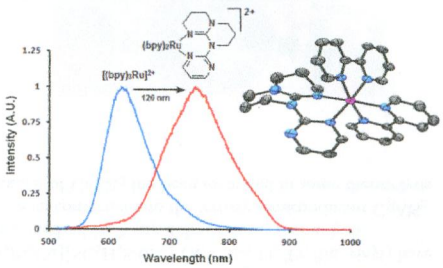

1690 Ⓢ dx.doi.org/10.1021/ic402836d

Reactions of $[PhI(pyridine)_2]^{2+}$ with Model Pd and Pt II/IV Redox Couples

Robert Corbo, Dayne C. Georgiou, David J. D. Wilson, and Jason L. Dutton*

The results of the reactions of the dicationic iodine(III) family of oxidants $[PhI(pyridine)_2]^{2+}$ with model Pd(II) and Pt(II) complexes are described. Depending on the specific reaction pairs, a variety of outcomes are observed; in general, oxidation of Pd(II) complexes to Pd(IV) results in immediate reduction back to Pd(II) with C−N or C−C bond formation. However, dicationic Pt(IV) complexes can be isolated.

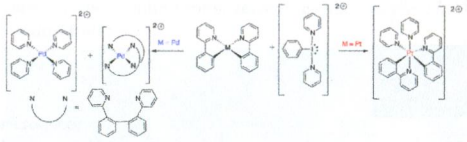

1699 Ⓢ dx.doi.org/10.1021/ic402838y

Dinuclear Pyridine-4-thiolate-Bridged Rhodium and Iridium Complexes as Ditopic Building Blocks in Molecular Architecture

Montserrat Ferrer,* Daniel Gómez-Bautista, Albert Gutiérrez, José R. Miranda, Guillermo Orduña-Marco, Luis A. Oro, Jesús J. Pérez-Torrente,* Oriol Rossell, Pilar García-Orduña, and Fernando J. Lahoz

A series of new dinuclear pyridine-4-thiolato compounds $[M(\mu\text{-}4\text{-}Spy)(diolef)]_2$ (M = Rh, Ir; diolef = cod, nbd) were used as ditopic building blocks for the construction of homo- and heterometallic rectangular assemblies composed of alternating dinuclear (Rh_2 or Ir_2) and mononuclear (Rh, Ir, Pd, or Pt) corners supported by four pyridine-4-thiolate linkers. These metallocycles are stereochemically nonrigid in solution, and their fluxional behavior was studied by variable-temperature NMR spectroscopy.

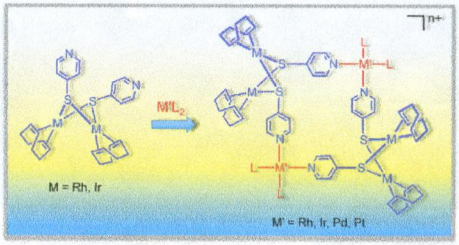

1712 Ⓢ dx.doi.org/10.1021/ic402784c

Excellent Selectivity for Actinides with a Tetradentate 2,9-Diamide-1,10-Phenanthroline Ligand in Highly Acidic Solution: A Hard−Soft Donor Combined Strategy

Cheng-Liang Xiao, Cong-Zhi Wang, Li-Yong Yuan, Bin Li, Hui He, Shuao Wang, Yu-Liang Zhao, Zhi-Fang Chai,* and Wei-Qun Shi*

A 2,9-diamide-1,10-phenanthroline ligand with hard−soft donors combined in the same molecule was designed for the group separation of actinides over lanthanides. The synthesis and solvent extraction as well as behaviors of complexation of the ligand with actinides and lanthanides are studied experimentally and theoretically. The ligand exhibits excellent complexation ability and high selectivity toward hexavalent, tetravalent, and trivalent actinides over lanthanides in highly acidic solution.

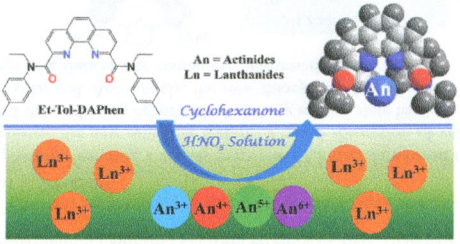

1721 S dx.doi.org/10.1021/ic402860r

Synthesis, Structure and Cation-Binding Properties of Some [4 + 4] Metallocyclic MO_2^{2+} (M = Mo or W) Derivatives of 9-Phenyl-2,3,7-trihydroxyfluor-6-one

Laura J. McCormick, Brendan F. Abrahams,* Berin A. Boughton, Martin J. Grannas, Timothy A. Hudson, and Richard Robson*

A series of ionic compounds involving anionic square-shaped $[(MO_2)_4Z_4]^{4-}$ metallocycles (M = Mo, W) (where Z^{3-} is the anion derived from 9-phenyl 2,3,7-trihydroxyfluor-6-one) is described. The metallocycles with an approximate edge length of almost 13 Å possess square cavities that are occupied by countercations in the solid state. ESI mass spectrometry indicates both tetra-anionic and trianionic metallocycles, the latter associated with an organic cation.

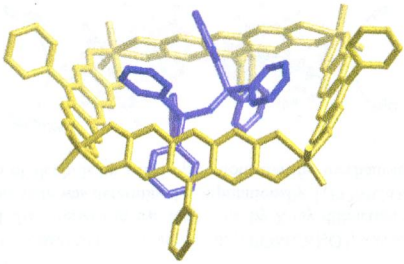

1729 S dx.doi.org/10.1021/ic402865p

Controllable Formation of Heterotrimetallic Coordination Compounds: Systematically Incorporating Lanthanide and Alkali Metal Ions into the Manganese 12-Metallacrown-4 Framework

Michael R. Azar, Thaddeus T. Boron III, Jacob C. Lutter, Connor I. Daly, Kelcie A. Zegalia, Ruthairat Nimthong, Gregory M. Ferrence, Matthias Zeller, Jeff W. Kampf, Vincent L. Pecoraro,* and Curtis M. Zaleski*

Crystal structures of 13 $Ln^{III}M^{I}(OAc)_4[12\text{-}MC_{Mn^{III}(N)shi}\text{-}4]$ complexes, where $^{-}$OAc is acetate, shi^{3-} is salicylhydroximate, M^{I} is Na^{I} or K^{I}, and Ln^{III} ranges from Pr^{III} to Yb^{III} (except Pm^{III}) and Y^{III}, demonstrate the controllable formation of heterotrimetallic compounds. The doming of the metallacrown ring can be explained through displacement of the ring metals toward one face of the macrocycle.

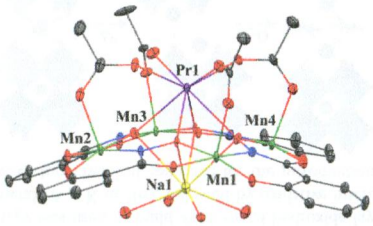

1743 dx.doi.org/10.1021/ic4028749

Applying the Fe(III) Binding Property of a Chemical Transferrin Mimetic to Ti(IV) Anticancer Drug Design

Timothy B. Parks, Yahaira M. Cruz, and Arthur D. Tinoco*

In the proposed Ti(IV)-based anticancer drug design strategy, the metal affinity properties of chemical transferrin mimetic (cTfm) ligands will be exploited to transport Ti(IV) into cells and release the metal by binding and depleting Fe(III). The ligands work in synergism with Ti(IV) to trigger cytotoxicity. Kinetic and cytotoxicity studies with *N,N′*-di(*o*-hydroxybenzyl)ethylenediamine-*N,N′*-diacetic acid (HBED), a cTfm representative, reveal the physiological feasibility of the drug design strategy and the specificity of the strategy for Ti(IV) activity.

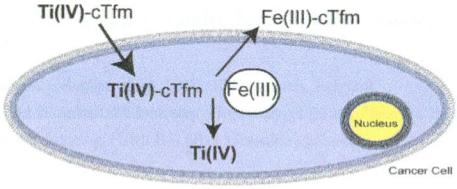

1750 dx.doi.org/10.1021/ic402877a

Structural and Spectroscopic Studies of Fluoroprotactinates

Stéphanie M. De Sio and Richard E. Wilson*

Seven protactinium(V) fluoro compounds have been synthesized, and their crystal structures and Raman spectra are reported. A comparison of the solid- and solution-state Raman spectra of these Pa fluoro compounds suggests that the Pa is eight-coordinate in aqueous hydrofluoric acid solution.

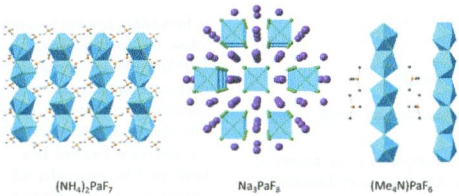

1756 dx.doi.org/10.1021/ic4028942

Explorations of New Second-Order Nonlinear Optical Materials in the Ternary Rubidium Iodate System: Noncentrosymmetric β-$RbIO_3(HIO_3)_2$ and Centrosymmetric $Rb_3(IO_3)_3(I_2O_5)(HIO_3)_4(H_2O)$

Xiang Xu, Bing-Ping Yang, Chao Huang, and Jiang-Gao Mao*

Two new rubidium iodates, β-$RbIO_3(HIO_3)_2$ ($P1$) and $Rb_3(IO_3)_3(I_2O_5)(HIO_3)_4(H_2O)$ ($P2_1/c$), have been synthesized and structurally characterized. A large bulk crystal of β-$RbIO_3(HIO_3)_2$ with dimensions of several millimeters has been grown. The crystal of β-$RbIO_3(HIO_3)_2$ possesses a short-wavelength absorption edge onset at 305 nm. Powder second-harmonic generation (SHG) measurements on sieved crystals reveal that β-$RbIO_3(HIO_3)_2$ is a type I phase-matchable material with an SHG response about 1.5 times that of KH_2PO_4.

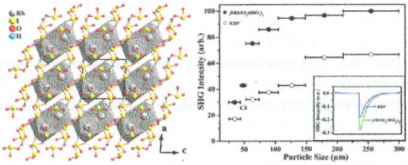

1764 S dx.doi.org/10.1021/ic402897d

A Comparative Insight of Potassium Vanadates as Positive Electrode Materials for Li Batteries: Influence of the Long-Range and Local Structure

Rita Baddour-Hadjean,* Arezki Boudaoud, Stéphane Bach, Nicolas Emery, and Jean-Pierre Pereira-Ramos

Three potassium vanadates have been prepared via a fast and facile solution route and applied as positive electrode materials in rechargeable Li batteries. Raman spectra and electrochemical performance are in line with their tunnel or layered framework. Among them, the double-sheet $K_{0.5}V_2O_5$ bronze is a new cathode, the best among the potassium–vanadium bronzes and oxides, with a reversible capacity of 210 mAh g^{-1} and excellent cycle life.

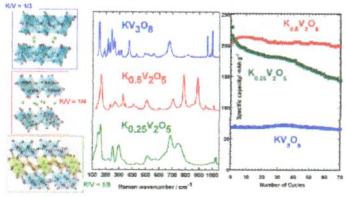

1773 S dx.doi.org/10.1021/ic402957c

Topochemical Synthesis of Alkali-Metal Hydroxide Layers within Double- and Triple-Layered Perovskites

Dariush Montasserasadi, Debasish Mohanty, Ashfia Huq, Luke Heroux, Edward Andrew Payzant, and John B. Wiley*

A two-step topochemical reaction strategy was used to build alkali-metal hydroxide layers within receptive perovskite hosts. Reductive intercalation with an alkali-metal (A = K or Rb), followed by oxidative intercalation with water, leads to CsCl-like A–OH layers. This method is an effective topochemical approach for the introduction of oxide species.

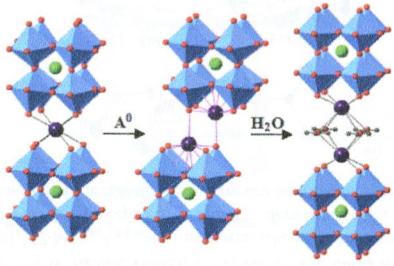

1779 S dx.doi.org/10.1021/ic402962c

Dicobalt-μ-oxo Polyoxometalate Compound, $[(\alpha_2\text{-}P_2W_{17}O_{61}Co)_2O]^{14-}$: A Potent Species for Water Oxidation, C–H Bond Activation, and Oxygen Transfer

Delina Barats-Damatov, Linda J. W. Shimon, Lev Weiner, Roy E. Schreiber, Pablo Jiménez-Lozano, Josep M. Poblet, Coen de Graaf, and Ronny Neumann*

A dimeric polyoxometalatate-based bis cobalt(III)-oxyl compound, $[(POMCo)_2O]$, was isolated by oxidation of a monomeric cobalt(II) precursor with ozone and characterized in the solid state by X-ray diffraction and in solution by multiple spectroscopic methods. The electronic state was determined computationally. $[(POMCo)_2O]$ was shown to be competent for the oxidation of water, the oxidation of alcohols by a hydrogen atom transfer mechanism, and oxygen transfer to sulfides as well a manganese porphyrin.

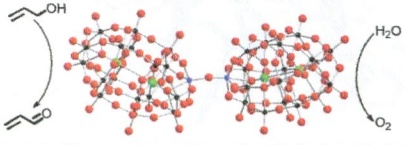

Additions and Corrections

1788 dx.doi.org/10.1021/ic5001039

Correction to Quantitative Vibrational Dynamics of the Metal Site in a Tin Porphyrin: An IR, NRVS, and DFT Study

Bogdan M. Leu,* Marek Z. Zgierski, Christian Bischoff, Ming Li, Michael Y. Hu, Jiyong Zhao, Steve W. Martin, Esen Ercan Alp, and W. Robert Scheidt

1789 dx.doi.org/10.1021/ic5000167

Correction to Synthesis and Properties of the Cyano Complex of Oxo-Centered Triruthenium Core $[Ru_3(\mu_3\text{-}O)(\mu\text{-}CH_3COO)_6(pyridine)_2(CN)]$

Hua-Xin Zhang,* Yoichi Sasaki,* Yi Zhang, Shen Ye, Masatoshi Osawa, Masaaki Abe, and Kohei Uosaki

Supporting Information available via online article